CHEMIJA
2025. Vol. 36. No. 4. P. 255–264

ISSN 0235-7216 eISSN 2424-4538
DOI: https://doi.org/10.6001/chemija.2025.36.4.5

Efficient photo-Fenton degradation of PAHs and PCBs in landfill leachate using Fe-CoBDC@Fe_3O_4 catalyst synthesised from recycled PET

Quoc Hai Nguyen[1*],

Thi Xuan Quynh Nguyen[2],

Luan Tran Ngoc Bao[2],

Hai D. Tran[2],

Nguyen Cong Nguyen[3],

Thong Ho Chi[4]

[1] Group of Applied Research in Advanced Materials for Sustainable Development, Faculty of Applied Sciences, Ton Duc Thang University, Ho Chi Minh City, Vietnam

[2] Ho Chi Minh City University of Natural Resources and Environment, 236B Le Van Sy Street, Tan Son Hoa Ward, Ho Chi Minh City, Vietnam

[3] Faculty of Chemistry and Environment, Dalat University, Da Lat City, Lam Dong Province, Vietnam

[4] University of Technology (HUTECH), 475A Dien Bien Phu Street, Thanh My Tay Ward , Ho Chi Minh City, Vietnam

Landfill leachate is highly challenging to treat due to its complex and unstable composition, containing high concentrations of ammonia nitrogen, chemical oxygen demand (COD), heavy metals, and persistent organic pollutants such as polyaromatic hydrocarbons (PAHs) and polychlorinated biphenyls (PCBs). In this study, a novel heterogeneous photo-Fenton catalyst, Fe-CoBDC@Fe_3O_4, was synthesised via a thermosolvent method using terephthalic acid regenerated from PET waste. The catalyst was employed for the degradation of recalcitrant compounds in leachate following pretreatment with an activated solid reactor. Upon UV irradiation (240 nm), the Fe-CoBDC@Fe_3O_4 catalyst generates electron–hole pairs, where the holes (h^+) oxidise water or hydroxyl ions (OH^-) to form hydroxyl radicals (•OH), which in turn degrade organic pollutants. Optimal treatment conditions were identified as a catalyst dosage of 1 g/L, H_2O_2 dosage of 0.8 mL, pH 3.0, and a reaction time of 30 min. Under these conditions, the removal efficiency of 97% for COD, 85% for PAHs and 84% for PCBs was achieved. These results demonstrate that Fe-CoBDC@Fe_3O_4 is a highly effective and sustainable photo-Fenton catalyst for the treatment of refractory compounds in industrial leachate.

Keywords: landfill leachate, PAHs, PCBs, heterogeneous photo-Fenton, catalyst

INTRODUCTION

The leachate composition is usually unstable and varies according to the landfill time, the type of waste, seasonal weather variations, the precipitation level and landfill temperature. All these factors make leachate treatment difficult and complicate [1]. It is a highly toxic liquid with heavy metals, different soluble materials and dissolving organic compounds such as pH, COD, BOD_5, suspended solids (SS), ammonium nitrogen (NH_3-N) and total Kjeldahl nitrogen (TKN), especially in

* Corresponding author. Email: nguyenquochai@tdtu.edu.vn

particular significant quantities of humic acid and fulvic as refractory organic pollutants [1, 2]. Others such as especially non-biodegradable organic matter, polyaromatic hydrocarbons (PAHs) with 0.85 to 1.47 mg/L and polychlorinated biphenyls (PCBs) with 0.01 to 0.08 mg/L, are among the most hazardous contaminants [3]. PCBs and PAHs are highly bioaccumulative and persistent, and their teratogenic, carcinogenic and endocrine-disrupting features have been widely reported in the literature. They are the environmental contamination mainly which is awful to human health. PCBs are organochlorine aromatic compounds classified as persistent organic pollutants and as carcinogenic to humans [4]. PAHs are a unique class of organic pollutants containing two or more fused aromatic rings, which are toxic and potential carcinogens [5]. PAHs are ubiquitous in the environment, either as a natural component, as products of humus conversion by microorganism organic materials, in particular during waste utilisation and house heating [6].

Conventional landfill leachate treatment methods fall into three main categories: (a) leachate transfer through recycling or co-treatment with domestic wastewater, (b) biological processes including aerobic and anaerobic degradation, and (c) physicochemical techniques such as oxidation, adsorption, precipitation, coagulation/flocculation, sedimentation/flotation, and air stripping [1]. However, the effectiveness of these approaches is increasingly challenged by the presence of poorly biodegradable organic inhibitors and heavy metals in leachate, which can hinder treatment performance and lead to elevated pollutant levels in the final effluent [7]. Several lab- and industrial-scale studies have demonstrated the effectiveness of membrane technology in removing pollutants from landfill leachate, achieving COD and heavy metal rejection rates above 98–99% [8, 9]. However, key challenges remain, including membrane fouling and the generation of large volumes of concentrate.

Chemical oxidation is a well-established approach for treating effluents containing refractory compounds, such as landfill leachate, due to its effectiveness in breaking down persistent pollutants resistant to conventional methods. In this study, we focus on advanced oxidation processes (AOPs) to enhance the removal efficiency of hazardous contaminants, particularly PAHs and PCBs, from landfill leachate. Most advanced oxidation processes, except for simple ozonation (O_3), involve the combination of strong oxidants such as O_3 and H_2O_2 with irradiation methods (e.g. ultraviolet (UV), ultrasound (US), or electron beam (EB)) and catalysts (e.g. transition metal ions or photocatalysts). A variety of AOPs have been extensively reviewed in recent literature. Typical systems include those involving irradiation, such as O_3/ultraviolet (UV) and H_2O_2/UV. In the H_2O_2/UV process, hydroxyl radicals (•OH) are generated through homolytic cleavage of the oxygen–oxygen bonds in hydrogen peroxide when exposed to UV light with a wavelength below 300 nm [10–13].

AOPs can be broadly categorised into four groups based on the use of irradiation and catalyst type: (i) AOPs with irradiation: These include methods such as electron beam, ultrasound (US), H_2O_2/US, UV/US, and photo-Fenton (H_2O_2/Fe^{2+}/UV). These processes are effective in generating hydroxyl radicals under irradiation for degrading persistent pollutants. (ii) AOPs without irradiation: Examples include O_3/H_2O_2, O_3/OH^-, and the classic Fenton process (H_2O_2/Fe^{2+}). These methods are widely applied in treating complex industrial wastewater containing contaminants such as phenols, nitrophenols, polychlorinated biphenyls (PCBs), dyes and formaldehyde [14, 15]. (iii) Heterogeneous AOPs without irradiation: An example is the electro-Fenton process, which relies on the electrochemical generation of reagents to drive oxidation without the need for light [16]. These AOPs are often used as tertiary treatment steps before effluent discharge into the environment. However, their effectiveness can vary, and treatment efficiency for stabilised landfill leachates is sometimes only moderate [17].

Polyethylene terephthalate (PET) contains up to 85% terephthalic acid (H_2BDC), making it a valuable precursor for synthesising metal-organic frameworks (MOFs), where H_2BDC serves as an ideal organic link [18]. In this study, we aimed to upcycle non-biodegradable PET waste into eco-friendly materials by recovering terephthalic acid from discarded plastic bottles to synthesise cobalt-based MOFs (CoBDC). Those MOFs were then explored as novel catalysts for chemical reactions. The catalytic efficiency of MOFs is attributed to their highly porous structure, large

surface area and well-defined framework, which promote the adsorption and activation of organic molecules [19, 20]. Such properties make them highly promising candidates for catalytic degradation processes, offering a sustainable approach to both waste valorization and environmental remediation. Catalytic activity of MOFs depends on the nature of the central metal ion. In order to increase the processing efficiency in the direction of combining the inherent pigment adsorption of MOFs and the degradation of molecules that have been adsorbed by AOPs, the authors introduced transition metals, the most common of which is Fe, into the frame structure of the material to create a Fenton photocatalytic effect [21].

This study aims to develop an effective treatment method for landfill leachate containing persistent organic pollutants such as PAHs and PCBs. The proposed approach integrates the high adsorption capacity of metal-organic frameworks (MOFs) with the oxidative power of advanced oxidation processes (AOPs). To induce the photo-Fenton catalytic effect, iron (Fe) ions were incorporated into the MOF framework by partially replacing cobalt salts during synthesis. The magnetic CoBDC MOFs were synthesised from terephthalic acid recovered from recycled PET waste, promoting sustainability in material sourcing. The Fe-doped MOFs will be systematically evaluated for their ability to degrade organic contaminants under various operational conditions, with a focus on elucidating the degradation mechanism, optimising treatment parameters, and assessing the material's reusability for long-term application in wastewater treatment.

MATERIALS AND METHODS

Materials

The chemicals utilised in this study included solid sodium hydroxide (NaOH), hydrochloric acid (HCl) and dimethylformamide concentrate (DMF), along with iron(II) chloride tetrahydrate ($FeCl_2.4H_2O$, purity > 99%) and iron(III) chloride hexahydrate ($FeCl_3.6H_2O$, purity > 99%). Additional reagents comprised dichloromethane (DCM, sourced from a domestic supplier in Vietnam), cobalt(II) chloride hexahydrate ($CoCl_2.6H_2O$, purity > 99.5%) and post-consumer polyethylene terephthalate (PET) plastic bottles. All chemicals were of analytical grade and primarily procured from reputable suppliers such as Merck (Germany), Xilong Scientific (China) and Sigma-Aldrich, through authorised distributors including Viet Hoa Chemical Co., Ltd. and Nam Phat Chemical in Ho Chi Minh City.

The leachate used for experimentation was collected from the reservoir at the Quang Trung landfill, located in Dong Nai Province, in March 2024. The sample was taken after the sedimentation tank, following the activated sludge treatment stage. Parameters including COD, PAHs, PCBs and pH were analysed and are summarised in Table 1.

Synthesis of materials

Synthesis of terephthalic acid from PET plastic bottles

Terephthalic acid (H_2BDC) was synthesised from recycled polyethylene terephthalate (PET) plastic bottles, following the procedure adapted from Sepehrmansourie et al. (2021) [22]. First, used PET bottles were shredded into fine fragments approximately 1 × 1 mm in size. A mixture of sodium hydroxide (NaOH) and PET was prepared in a glass beaker such that the molar ratio of NaOH to PET was maintained at 3:1. To this mixture, 80 mL of distilled water was added, and the solution was heated under continuous stirring. As the reaction progressed, the PET gradually decomposed, forming a milky white suspension, indicating the formation of sodium terephthalate. Subsequently, 200 mL of additional distilled

Table 1. **Characteristics of landfill leachate at Quang Trung, Vietnam**

No.	Parameters	Unit	Leachate after activated sludge reactor	Average
1	COD	mg/L	1328.52–1825.68	1560
2	PAHs	mg/L	0.98–2.58	1.8
3	PCBs	mg/L	0.02–1.07	0.8
4	pH	–	7.1–8.5	7.8

water was introduced to facilitate the separation of sodium terephthalate from any undissolved residues. The mixture was then filtered to remove solid impurities, and the clear filtrate was collected. Concentrated hydrochloric acid (HCl) was slowly added to the filtrate until a white precipitate of terephthalic acid formed and the pH of the solution reached approximately 2. The precipitate was separated by filtration and thoroughly washed with 500 mL of distilled water until the washings reached a neutral pH of 6–7. Finally, the purified precipitate was dried at 100°C until a constant mass was achieved, yielding white crystalline terephthalic acid suitable for subsequent use.

Synthesis of Fe_3O_4

A mixture of $FeCl_3.6H_2O$ and $FeCl_2.4H_2O$ in a 2:1 molar ratio is dissolved in 100 mL of distilled water and stirred at 80°C for 30 min. A NaOH solution is then added dropwise until pH reaches 10, and the reaction mixture is maintained for additional 30 min. The resulting precipitate is collected using a magnet and washed several times with water and ethanol until the pH stabilises between 6 and 7. Finally, the product is dried at 60°C for 8 h to obtain Fe_3O_4 nanoparticles.

Synthesis of CoBDC, CoBDC@Fe_3O_4 and Fe-CoBDC@Fe_3O_4 composites

The CoBDC materials were synthesised according to the procedure described, with the quantities of reagents detailed in Table 2. For the synthesis of CoBDC@Fe_3O_4 and Fe-CoBDC@Fe_3O_4, the required amount of Fe_3O_4 (0.214 g) was first dispersed in 50 mL of deionized water and ultrasonicated for 2 h to obtain a homogeneous suspension. In parallel, a mixture of H_2BDC (2 g), $CoCl_2.6H_2O$, and, when applicable $FeCl_3.6H_2O$, was dissolved in 90 mL of DMF under magnetic stirring. The two solutions were combined and further sonicated for 1 h, then transferred into a sealed reaction vessel and heated at 100°C for 24 h. Upon cooling to room temperature, the resulting solids were separated by decanting the supernatant. The products were purified by sequential soaking in DMF and DCM, each solvent used three times (10 mL per cycle), with each soaking step lasting 24 h. After each cycle, the solvent was removed and replaced with a fresh solvent to ensure the complete removal of unreacted precursors and impurity.

Lab-scale experiment

The photocatalytic experiments were conducted at room temperature using a simple cylindrical beaker-type reactor with a capacity of 500 mL (Fig. 1). A Fe-CoBDC@Fe_3O_4 photocatalyst was putted in a reactor, while a UV lamp controlled by an external DC digital UV generator was placed inside the reactor. The solution was continuously agitated using a magnetic stir bar at a moderate speed of 20–25 rpm to ensure a uniform mixing without inducing vortex formation. A 500 mL volume of synthetic wastewater was introduced into the reactor. The UV generator was then activated, delivering an intensity range of 500–1000 W with emission wavelengths between 200 and 280 nm. The photocatalytic treatment was monitored over a time span of 10 to 50 min, targeting the

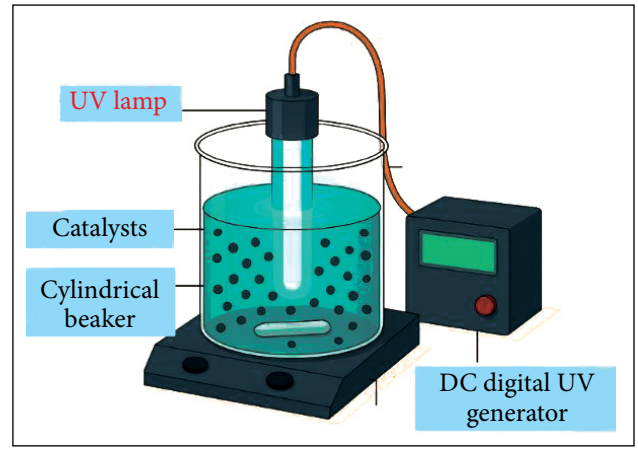

Fig. 1. Schematic diagram of the experimental system for the heterogeneous photo-Fenton catalytic reaction

Table 2. **Compositions used for the synthesis of CoBDC-based materials**

Material	$FeCl_3{\cdot}6H_2O$, g	$CoCl_2{\cdot}6H_2O$, g	H_2BDC, g	Fe_3O_4, g
CoBDC	0	2.408	2	0
CoBDC@Fe_3O_4	0	2.408	2	0.214
Fe-CoBDC@Fe_3O_4	0.282	2.164	2	0.214

degradation of COD, PAHs and PCBs. The Fe-CoBDC@Fe_3O_4 catalyst (applied at 1 mg/L) features a three-dimensional spatial framework in which partial substitution of Co^{2+} by Fe^{3+} occurs at the coordination nodes. This structural configuration imparts a semiconductor-like behaviour to the material. Specifically, the empty d-orbitals of Fe ions, bridged by organic ligands, contribute to the formation of a conduction band, enhancing the catalyst's electron mobility and photocatalytic performance under UV irradiation [22, 23]. Before UV irradiation, the catalyst–wastewater suspension was stirred in the dark for 30 min to achieve the adsorption–desorption equilibrium between pollutants and the catalyst surface. This control step confirmed that pollutant removal in the absence of light was negligible, thus verifying the photocatalytic nature of the degradation process.

Photocatalytic mechanism of Fe-CoBDC@Fe_3O_4 in the heterogeneous photo-Fenton system

Upon exposure to UV light with photon energies equal to or exceeding the bandgap of the material, the Fe-CoBDC@Fe_3O_4 catalyst undergoes electronic excitation. Specifically, electrons (e^-) are excited from the valence band to the Fe^{3+} conduction band, leaving behind holes (h^+) in the valence band. These photogenerated electrons (e_{cb}^-) readily react with externally supplied H_2O_2 (in a range of 0.1–1.5 mM), producing hydroperoxyl radicals (•OOH) and Fe^{2+} ions, as illustrated in Eq. (1). During this process, a portion of Fe in the Fe-CoBDC@Fe_3O_4 framework may be consumed:

$$e_{cb}^- + H_2O_2 \rightarrow \bullet OOH + OH^- + Fe^{2+}. \quad (1)$$

The Fe^{2+} thus generated further reacts with residual H_2O_2 to produce Fe^{3+} and hydroxyl radicals (•OH), as shown in Eq. (2):

$$Fe^{2+} + H_2O_2 \rightarrow Fe^{3+} + \bullet OH + OH^-. \quad (2)$$

The highly oxidative •OH radicals formed in Eqs. (2) and (3) serve as the principal agents in the mineralisation of complex organic pollutants such as COD, PAHs and PCBs into harmless end-products like CO_2 and H_2O. This efficient generation of reactive oxygen species (ROS) highlights the superior photocatalytic activity of Fe-CoBDC@Fe_3O_4 under UV irradiation. The reaction kinetics and rate constants for the photodegradation of these organic compounds using Fe-CoBDC@Fe_3O_4 are currently under investigation.

Analytical methods

The pH of the solution was continuously monitored using a digital pH meter (HANNA HI 991001) to ensure optimal reaction conditions. Chemical Oxygen Demand (COD) concentrations were determined in accordance with the Standard Methods for the Examination of Water and Wastewater, specifically Section 5220 B:2017. The concentrations of polycyclic aromatic hydrocarbons (PAHs) and polychlorinated biphenyls (PCBs) were quantified following Section 5120 B:2017, using Gas Chromatography–Mass Spectrometry (GC–MS) as the analytical technique [24]. The concentration of hydrogen peroxide (H_2O_2) was measured using a colorimetric method based on the formation of a yellow complex between H_2O_2 and titanium (IV) ions. In this method, a $Ti(SO_4)_2$ solution in sulfuric acid (H_2SO_4) was used as the complexing agent, and

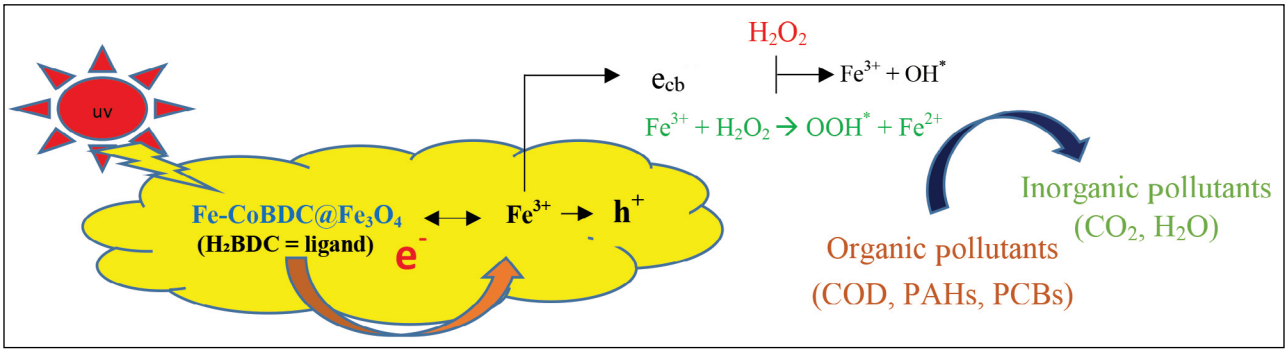

Fig. 2. Schematic representation of the photocatalytic degradation mechanism via the heterogeneous photo-Fenton process

the absorbance of the resulting peroxytitanium complex was recorded at 420 nm.

RESULTS AND DISCUSSION

Effects of UV energy

Fe-CoBDC@Fe_3O_4 material three-dimensional spatial structure has the empty d orbitals of iron interlaced by organic ligands forming the conduction region which favours the absorption of UV with the variation of agreeable UV [25, 26]. The organic ligands absorb the wavelength energy, with UV 240 nm, produce more e^- and d orbitals of iron to produce h^+ and e_{cb}^- (Eq. (3)). Furthermore, the combination e_{cb}^-, Fe^{3+} and H_2O_2 added form outside as catalysts create HOO• and Fe^{2+} (Eq. (4)), which exhibit better catalytic activities to create •OH radicals (Eqs. (4, 5)) removing the efficiency of organic pollutants and the single Fe(III) ions concentration max [27]. The photolytic induced oxidation with ozone or hydrogen peroxide needs UV with wavelengths below 300 nm [49]:

$$\text{Ligand} + h\nu \rightarrow e_{cb}- + h^+, \quad (3)$$

$$H_2O_2 + e_{cb}^- + Fe^{3+} \rightarrow \bullet OOH + Fe^{2+}, \quad (4)$$

$$H_2O_2 + \bullet OOH + Fe^{2+} \rightarrow Fe^{3+} + \bullet OH, \quad (5)$$

$$Fe^{3+} + \bullet OH + \text{Organic Pollutants (COD, PAHs, PCBs…)} \rightarrow \text{Inorganic Pollutants } (CO_2, H_2O \text{ and others}). \quad (6)$$

As shown in Fig. 3, the variations in Fe^{3+} and Fe^{2+} concentrations under different irradiation wavelengths indicate that the Fe^{3+}/Fe^{2+} ratio is strongly dependent on the incident light energy. Those batch experiments were designed to examine how light energy influences the photo-induced redox conversion of iron species. Each wavelength corresponds to its experimentally determined optimal irradiation time (200 nm – 10 min, 220 nm – 20 min, 240 nm – 30 min, 260 nm – 40 min, 280 nm – 50 min), representing the steady-state Fe^{3+}/Fe^{2+} conditions used for comparison. The combination of Fe^{3+} with H_2O leads to the formation of $Fe(OH)_2^+$ and H^+ (Eqs. (7, 8)), illustrating that the heterogeneous photo-Fenton reaction involves a synergy between Fenton reagents and the incident light energy ($\lambda < 580$ nm). Under these conditions, the maximum concentration of Fe(II) ions is produced, and the Fe^{3+} to Fe^{2+} ratio approaches 1:1 ($\lambda < 240$ nm). In this environment, $Fe(OH)_2^+$ and H_2O_2 interact with UV light, generating the dominant hydroxyl radical (•OH). Furthermore, at $\lambda < 310$ nm, the photolysis of hydrogen peroxide leads to the formation of •OH radicals (Eq. (9)), which are fundamentally tied to redox processes. At alkaline pH levels, UV light

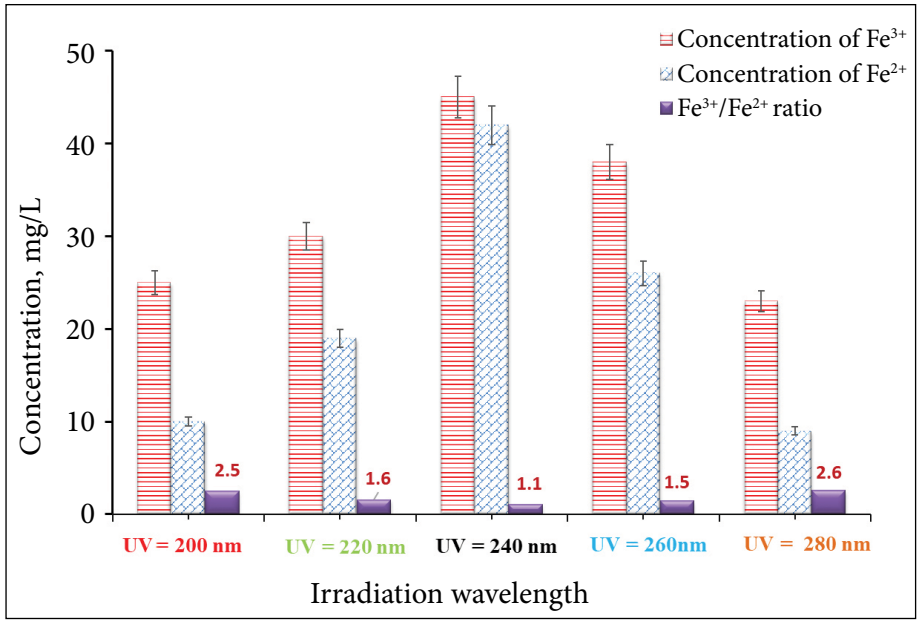

Fig. 3. Effect of the irradiation wavelength on Fe^{2+} and Fe^{3+} concentrations and the Fe^{3+}/Fe^{2+} ratio, which governs the efficiency of the photo-Fenton reaction

acts as a catalyst for the nondissociated molecules of H_2O_2 and H^+ (Eq. (10)), resulting in the formation of OH^-. Consequently, high energy is required when organic or inorganic pollutants in wastewater strongly absorb UV radiation. Moreover, H_2O_2 dissociates into H^+, as shown in Eq. (11), which counters the increase in alkalinity. The formation of HOO• in Eqs. (4) and (11) promotes UV absorption and generally enhances the production of •OH radicals (Eq. (12)). In short, the influence of UV energy on the creation of Fe^{3+}, Fe^{2+} and especially the Fe^{3+}/Fe^{2+} ratio. This enhances the ability of •OH to reduce pollutants, which suggests that the importance of UV energy has an effect to create •OH:

$$Fe^{3+} + H_2O \rightarrow Fe(OH)_2^+ + H^+, \quad (7)$$

$$Fe(OH)_2^+ + h\nu \rightarrow Fe^{2+} + \bullet OH \ \mathbf{(\lambda < 580\ nm)}, \quad (8)$$

$$H_2O_2 + h\nu \rightarrow 2\bullet OH \ \mathbf{(\lambda < 310\ nm)}, \quad (9)$$

$$H_2O_2 + h\nu + H^+ \rightarrow H_2O + O_2 + OH^-, \quad (10)$$

$$H_2O_2 \rightarrow HOO\bullet + H^+, \quad (11)$$

$$H_2O_2 + h\nu + H^+ \rightarrow 2\bullet OH. \quad (12)$$

Effects of pH

In a heterogeneous photo-Fenton process, the initial pH plays a critical role as it controls the production of hydroxyl radicals and the concentration of ferrous ions [28]. This study investigated the effect of pH on pollutant reduction efficiency using the Fenton process (as shown in Fig. 4). A 500 mL sample of landfill leachate was acidified with HCl (0.02 M) to pH values ranging from 1 to 5. The experiments were conducted under UV irradiation at 240 nm for 50 min, while all other parameters were kept constant. When the pH ranged from 1 to 2, the removal efficiency of COD, PAHs and PCBs increased. This could be due to the combination of Fe^{3+} with H_2O, producing H^+ (Eq. (9)), and the reaction of H_2O_2 with UV light and H^+ to generate hydroxyl radicals (•OH) (Eq. (12)), which enhance the reduction of pollutant compounds. However, the concentration of H_2O_2 in the reaction system decreased significantly due to its reaction with H^+ to form oxonium ions ($H_3O_2^+$) (Eq. (13)) [29] or water (Eq. (14)) [30], particularly when excess H^+ was present in the solution (Eq. (10)):

$$H_2O_2 + H^+ \rightarrow H_3O_2^+, \quad (13)$$

$$H_2O_2 + 2H^+ + 2e^- \rightarrow 2H_2O. \quad (14)$$

This results in the reduction in the amount of •OH generated by the Fenton reaction (Eq. (9)). At pH 3, the apparent rate constant for oxidation reached its highest value, with the removal efficiencies of COD, PAHs and PCBs peaking at 97, 85 and 89%, respectively. This improvement is attributed to the neutralisation of H^+ and OH^- concentrations, which are produced by H_2O_2 and UV (Eq. (10)). Additionally, an acidic medium was created,

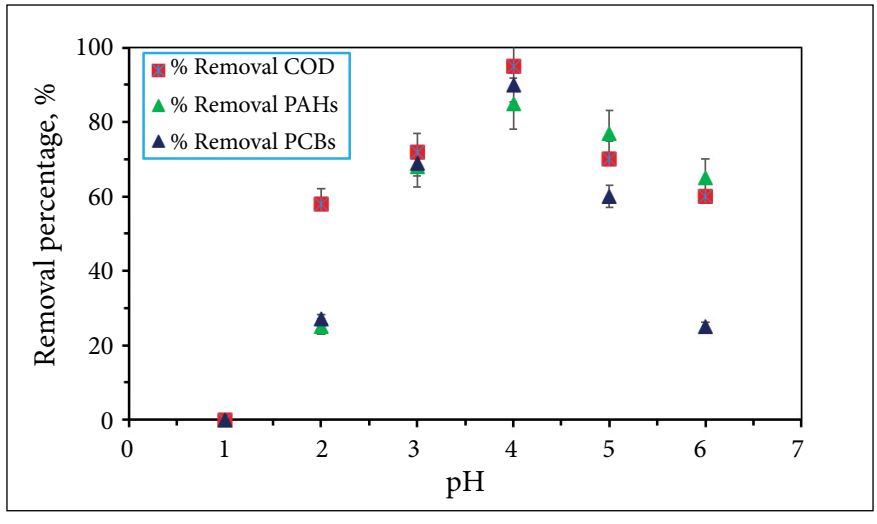

Fig. 4. The effect of pH on the removal efficiency of COD, PAHs and PCBs in landfill leachate was investigated under UV irradiation at 240 nm for 50 min

facilitating the hydrolysis of Fe^{3+} by H_2O to produce $Fe(OH)_2$, which readily generates •OH (Eq. (6)).

In contrast, at higher pH (pH > 3), the amount of H_2O_2 decreases due to its decomposition (Eq. (13)), leading to the formation of water and •OH radicals. These radicals react with Fe^{3+}, reducing it to Fe^{2+} (Eq. (14). The hydrolysis of Fe^{3+} by H_2O (Eq. (5)) produces $Fe(OH)_2$, which can precipitate and adhere to the cathode surface, preventing UV absorption by $Fe(OH)_2$ and hindering the regeneration of Fe^{2+} catalyst (Eq. (6)). Furthermore, an increase in pH can decrease the oxidation potential of the •OH radical, which in turn reduces the treatment efficiencies of COD, PAHs and PCBs [31]:

$$H_2O_2 + \bullet OH \rightarrow 4H_2O + \bullet HO_2, \quad (15)$$

$$Fe^{3+} + \bullet HO_2 \rightarrow 4Fe^{2+} + O_2 + H^+. \quad (16)$$

Effect of H_2O_2 dosage

The effect of H_2O_2 dosage on pollutant removal was examined under UV irradiation at 240 nm and pH = 3 in the batch mode, with reaction times ranging from 0 to 50 min, as shown in Fig. 5. The experiments were performed in the batch mode, using equal volumes of landfill leachate for all tests. Each experimental run was carried out independently for a specific reaction time (0, 10, 20, 30, 40 and 50 min). The H_2O_2 volume varied from 0.1 to 1.5 mL. The degradation efficiencies of COD, PAHs and PCBs increased rapidly within the first 20 min when the H_2O_2 dosage was between 0.1 and 0.56 mL. However, when the H_2O_2 volume exceeded 0.56 mL, the degradation efficiency gradually decreased beyond the 20-minute mark. The highest treatment efficiencies were observed at 97, 85 and 89% for COD, PAHs and PCBs, respectively, when 0.8 mL of H_2O_2 was used over a 30-minute period. Beyond this point, with H_2O_2 volumes exceeding 0.8 mL for 30 min, the excess of H_2O_2 was combined with hydroxyl radicals (•OH) to form water and hydroperoxyl radicals ($\bullet HO_2$), as shown in Eq. (13). This reaction led to a reduction in the available active •OH radicals, resulting in a decrease in treatment efficiency for COD, PAHs and PCBs [20]. The added H_2O_2 dosage and reaction time explain why Fe-CoBDC@Fe_3O_4 material, when illuminated by UV, exhibits higher processing efficiency compared to its behaviour in the dark. This enhanced efficiency is attributed to the photocatalytic mechanism activated by UV light. The presence of H_2O_2 further prevents electron–hole recombination (Eqs. (1, 2)), leading to increased photodegradation efficiency through the generation of additional •OH radicals [30, 31].

GC–MS analysis and photocatalytic degradation mechanism of PAHs and PCBs

GC–MS analysis revealed several intermediate peaks formed during the degradation of PAHs and PCBs under the heterogeneous photo-Fenton system. For PAHs, key intermediates such as 9-methylene-9H-fluorene, fluoranthene and 1,5-diphenyl-1,4-pentadiyn-3-one were detected, indicating

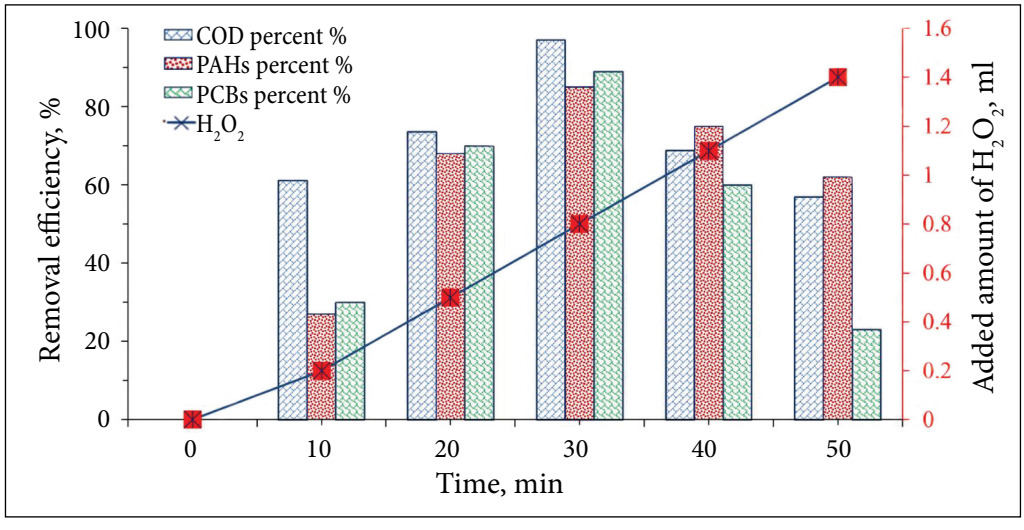

Fig. 5. Effect of the H_2O_2 dosage on the removal efficiency of COD, PAHs and PCBs in the landfill leachate under UV irradiation (240 nm) at pH = 3 for different reaction times

oxidative ring-opening and the formation of oxygenated products including ketones, quinones, aldehydes and low-ring furans [32]. In the case of PCBs, the degradation pathway involved hydroxylation and dechlorination, leading to the formation of intermediate peaks including alkanes, aldehydes, ketones and esters, as reported in a study utilising Fe_3O_4@β-CD/g-C_3N_4 as a photo-Fenton catalyst [6].These findings support a stepwise transformation of PCBs into lower molecular weight and more polar compounds, eventually resulting in the complete mineralisation into CO_2 and H_2O. To better visualize these transformation routes, a schematic degradation pathway of PAHs and PCBs under the photo-Fenton system is illustrated in Fig. 6. This figure summarises the main oxidation and dechlorination steps, showing how complex aromatic pollutants are gradually converted into oxygenated intermediates and ultimately mineralised to CO_2 and H_2O.

The combination of a strong adsorption from the MOF structure and the oxidative power of photo-generated hydroxyl radicals (•OH) accounts for the high removal efficiency. The Fe-CoBDC@Fe_3O_4 catalyst not only adsorbs pollutants effectively but also promotes their degradation through a continuous Fe^{2+}/Fe^{3+} cycling and photo-assisted radical generation. This dual-function mechanism confirms the potential of Fe-doped MOFs as a promising solution for treating landfill leachate containing persistent organic pollutants such as PAHs and PCBs.

CONCLUSIONS

Fe-CoBDC@Fe_3O_4 material is a composite of iron (Fe) and cobalt (Co) metal-organic frameworks (MOFs) with magnetite (Fe_3O_4), enhancing its photocatalytic activity. When exposed to UV light, electrons are excited from the valence band to the conduction band, creating electron–hole pairs. The holes (h^+) in the valence band have a strong oxidation capacity, allowing them to oxidise adsorbed organic molecules or hydroxyl ions (OH^-) to generate hydroxyl radicals (•OH). These radicals are highly reactive and can effectively degrade persistent organic pollutants such as COD, PAHs and PCBs in leachate. This study showed

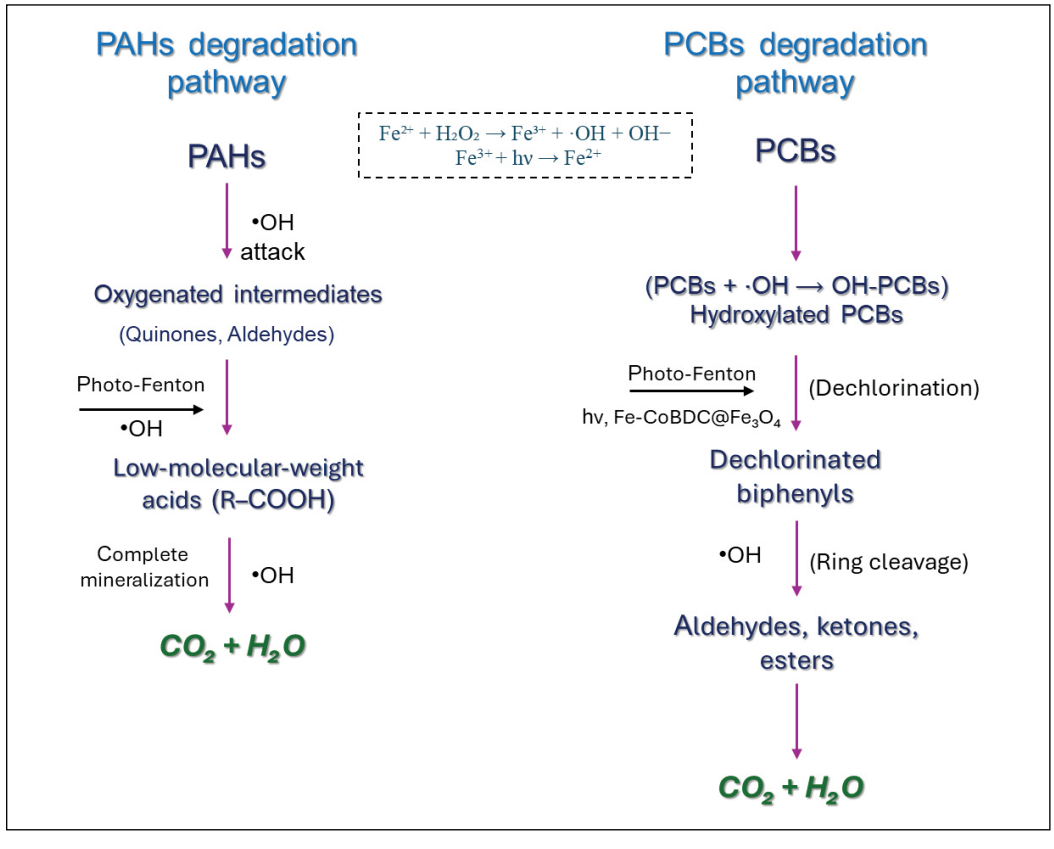

Fig. 6. Schematic degradation pathways of PAHs and PCBs under the Fe-CoBDC@Fe_3O_4 photo-Fenton system

that the optimal conditions – material loading of 1 g/L, dosage of H_2O_2 0.8 mL, pH 3.0 and contact time 30 min, with 240 nm UV and the combination of Fe-CoBDC@Fe_3O_4 material with an UV process – can effectively reduce the level of COD 97%, PAHs 85% and PCBs 84% landfill leachate. This demonstrates the significant potential of the Fe-CoBDC@Fe_3O_4 catalyst combined with UV light for treating landfill leachate, effectively breaking down harmful organic compounds.

ACKNOWLEDGEMENTS

This research was funded by the Ministry of Education and Training (Vietnam) under Project Code B2024-DLA-03.

Received 3 September 2025
Accepted 26 November 2025

References

1. S. Renou, J. G. Givaudan, S. Poulain, F. Dirassouyan, P. Moulin, *J. Hazard*. Mater., **150**, 468 (2008).
2. S. Cortez, P. Teixeira, R. Oliveira, M. Mota, *J. Hazard*. Mater., **182**, 730 (2010).
3. F. Wang, M. Gamal El-Din, D. W. Smith, *Ozone Sci. Eng*., **26**, 287 (2004).
4. K. Šrédlová, T. Cajthaml, *Chemosphere*, **287**, 132096 (2022).
5. A. B. Patel, S. Shaikh, K. R. Jain, C. Desai, D. Madamwar, *Front. Microbiol.*, **11**, 562813 (2020).
6. K. Srogi, *Environ. Chem. Lett*., **5**, 169 (2007)
7. F. Çeçen, Ö. Aktaş, *Environ. Eng. Sci*., **21**, 303 (2004).
8. K. Linde, A. Jönsson, R. Wimmerstedt, *Desalinatio*n, **101**, 21 (1995).
9. T. Bilstad, M. V. Madland, *Water Sci. Technol*., **25**, 117 (1992).
10. F. Wang, D. W. Smith, M. G. El-Din, *J. Environ. Eng. Sci*., **2**, 413 (2003).
11. P. Schulte, A. Bayer, F. Kuhn, T. Luy, M. Volkmer, *Ozone Sci. Eng*., **17**, 119 (1995).
12. N. H. Ince, *Water Environ*. Res., **70**, 1161 (1998).
13. A. Wenzel, A. Gahr, R. Niessner, *Water Res*., **33**, 937 (1999).
14. S. M. Kim, S. U. Geissen, A. Vogelpohl, *Water Sci. Technol*., **35**, 239 (1997).
15. S. H. Gau, F. S. Chang, *Water Sci. Technol*., **34**, 455 (1996).
16. C. P. Huang, C. Dong, Z. Tang, *Waste Manag*., **13**, 361 (1993).
17. A. C. Silva, M. Dezotti, G. L. Sant'Anna, *Chemosphere*, **55**, 207 (2004).
18. W. P. R. Deleu, I. Stassen, D. Jonckheere, R. Ameloot, D. E. DeVos, *J. Mater. Chem. A*, **4**, 9519 (2016).
19. J. Y. Lee, O. K. Farha, J. Roberts, K. A. Scheidt, S. B. T. Nguyen, J. T. Hupp, *Chem. Soc. Rev*., **38**, 1450 (2009).
20. J. A. Melero, G. Calleja, F. Martínez, R. Molina, M. I. Pariente, *Chem. Eng. J*., **131**, 245 (2007).
21. J. He, Y. Zhang, X. Zhang, Y. Huang, *Sci. Rep*., **8**, 1 (2018).
22. H. Sepehrmansourie, M. Zarei, M. A. Zolfigol, S. Babaee, S. Rostamnia, *Sci. Rep*., **11**, 1 (2021).
23. J. J. Du, Y. P. Yuan, J. X. Sun, et al., *J. Hazard. Mater*., **190**, 945 (2011).
24. K. Mastovska, S. J. Lehotay, *J. Chromatogr. A*, **1000**, 153 (2003).
25. M. B. Kasiri, H. Aleboyeh, A. Aleboyeh, *Appl. Catal. B Environ*., **84**, 9 (2008).
26. S. M. Kim, A. Vogelpohl, *Chem. Eng. Technol*., **21**, 187 (1998).
27. Y. Zhu, R. Zhu, Y. Xi, J. Zhu, G. Zhu, H. He, *Appl. Catal. B Environ*., **255**, 117739 (2019).
28. M. Zhou, Q. Yu, L. Lei, G. Barton, *Sep. Purif. Technol*., **57**, 380 (2007).
29. L. Lunar, D. Sicilia, S. Rubio, D. Pérez-Bendito, U. Nickel, *Water Res*., **34**, 1791 (2000).
30. H. K. Singh, M. Saquib, M. M. Haque, M. Muneer, *J. Hazard. Mater.*, **142**, 374 (2007).
31. R. Jain, M. Shrivastava, *J. Hazard. Mater*., **152**, 216 (2008).
32. X. Sun, Z. Ran, Y. Wu, et al., *RSC Adv.*, **12**, 7335 (2022).

Quoc Hai Nguyen, Thi Xuan Quynh Nguyen, Luan Tran Ngoc Bao, Hai D. Tran, Nguyen Cong Nguyen, Thong Ho Chi

EFEKTYVUS PAH IR PCB SKAIDYMAS SĄVARTYNO FILTRATE FOTOFENTONU, NAUDOJANT IŠ PERDIRBTO PET SUSINTETINTĄ Fe-CoBDC@Fe_3O_4 KATALIZATORIŲ